

Magnetic Phase Diagram of Weakly Pinned Type-II Superconductors

Satyajit Sukumar BANERJEE¹, Srinivasan RAMAKRISHNAN^{1,*}, Dilip PAL¹, Shampa SARKAR¹, Arun Kumar GROVER^{1,*}, Gurazada RAVIKUMAR², Prasant Kumar MISHRA², Turumella Venkata CHANDRASEKHAR RAO², Vinod Chandra SAHNI², Chakkalakal Varduuny TOMY³, Mark Joseph HIGGINS⁴ and Shobo BHATTACHARYA^{1,4}

¹ *Department of Condensed Matter Physics and Materials Science, Tata Institute of Fundamental Research, Mumbai-400005, India*

² *Technical Physics and Prototype Engineering Division, Bhabha Atomic Research Center, Mumbai-400085, India*

³ *Department of Physics, Indian Institute of Technology, Powai, Mumbai-400076, India.*

⁴ *NEC Research Institute, 4 Independence Way, Princeton, New Jersey 08540, U.S.A*

The phenomenon of superconductivity was discovered in 1911, however, the methodology to classify and distinguish type-II superconductivity was established only in late fifties after Abrikosov's prediction of a flux line lattice in 1957. The advent of high temperature superconductors (HTSC) in 1986 focused attention onto identifying and classifying other possible phases of vortex matter in all classes of superconductors by a variety of techniques. We have collated evidences in support of a proposal to construct a generic phase diagram for weakly pinned superconducting systems, based on their responses to ac and dc magnetic fields. The phase diagram comprises quasi-glassy phases, like, the Bragg glass, a vortex glass and a reentrant glass in addition to the (completely) amorphous phases of pinned and unpinned variety. The characteristic metastability and thermomagnetic history dependent features recognized amongst various glassy vortex phases suggest close connections between vortex matter and other disordered condensed matter systems, like, spin glasses, super cooled liquids/ structural glasses, etc. A novel quenched random disorder driven fracturing transition stands out amongst other noteworthy facets of weakly vortex pinned vortex matter.

PACS numbers : 64.70 Dv, 74.60 Ge, 74.25 Dw, 74.60 Ec, 74.60 Jg

I. INTRODUCTION

Superconducting materials in general are of two types, viz., (i) the type-I, which completely shield the external magnetic field (H) upto a limiting value called the *thermodynamic critical field* H_c , and (ii) the type-II, which completely shield the magnetic field (H) upto a threshold called the lower critical field ($H_{c1}(T)$) and above this field an incomplete shielding persists upto an upper critical field $H_{c2}(T)$, where the type-II superconductor turns normal. A phenomenological mean field description of the magnetic phase diagram of a type II superconductor, as proposed by A. A. Abrikosov [1] in 1957, comprises a mixed phase between $H_{c1}(T)$ and $H_{c2}(T)$, where the magnetic field resides inside the superconductor in the form of string like entities called *vortices*. Each vortex is associated with a quantum of flux, $\phi_0 = hc/2e$. The repulsive interaction between the vortices stabilizes them into a regular (generally hexagonal) periodic arrangement (often designated as the flux line lattice FLL) with an inter-vortex separation a_0 varying as $1/\sqrt{H}$, where H is the magnetic field. The penetration depth λ determines the range of the repulsive interaction between the vortices; the interaction falls off as $\exp(-r/\lambda)/\sqrt{r}$ at large distances (r) and it varies logarithmically at small distances [2]. The response of the FLL to stress, is similar to that of an elastic medium and one needs to associate three elastic moduli for the hexagonal symmetry of FLL (e.g.,

c_{11} (for compression), c_{44} (for tilt) and c_{66} (for shear)).

In realistic superconducting samples, the superconducting order parameter could get preferentially suppressed at locations of atomic inhomogeneities, which therefore become energetically favorable sites for the localization (i.e., pinning) of the normal core of any vortex. A measure of the pinning strength experienced by the vortex array is obtained via the material attribute *critical current density* (J_c) which can be defined as the maximum current that can be sustained by a superconductor without depinning the vortices (or loosing the zero resistance property).

Theoretical work of late eighties and nineties has shown that by taking into account the effects of thermal fluctuations and pinning centers on vortices, the mean field description of a type II superconductor gets substantially modified and new phases and phase boundaries of vortex matter have been predicted [3]. In particular, in 1988 D. R. Nelson [4] predicted that in a clean pinning free system, an ideal FLL phase is stable only in the intermediate field range under the influence of thermal fluctuations (see Fig.1(a) for a schematic plot). A new phase, viz., the *vortex liquid state*, in which the inter-vortex correlation length is of the order of a_0 , was predicted to exist at very low fields near H_{c1} and as well as at very high fields just before H_{c2} , such that the phase boundary marking the vortex solid to vortex liquid transformation is reentrant. This implies that while increasing

field at a fixed T , one should first encounter the dilute low density ($a_0 \gg \lambda$) vortex liquid phase, followed by an ideal FLL and, finally, one should reach a very dense ($a_0 \sim \xi$) vortex liquid phase. Experimental studies on high temperature superconductors (HTSC) have established the existence of vortex solid to liquid transition at high fields, however, the demonstration of the reentrant behavior of melting phase boundary at low fields has so far proved to be elusive. The mean field scenario predicts that a perfectly periodic arrangement of vortices (ideal FLL) should undergo a qualitative transformation under the influence of pinning centers such that the vortex lattice has spatial correlations only upto a limit as in a glassy phase [5]. The vortex glass phase can exhibit many metastable configurations, each of which is characterized by zero linear resistivity. In 1994, T. Giamarchi and P. Le Doussal [6] proposed the existence of a novel (vortex) solid to solid transformation as a function of varying field at a fixed temperature. In their framework, a novel Bragg glass (i.e., a quasi-FLL) phase at intermediate fields and weak disorder transforms (presumably via a first order transition) into a vortex glass state at high fields and stronger disorder. This solid to solid transformation (see Fig.1(b) for a schematic phase diagram) is considered to arise due to a proliferation of dislocations in the Bragg glass phase, which is initially assumed to be free of dislocations of any kind. A large fraction of the experimental efforts since the advent of HTSC era have focused on identifying the characteristics of different types of dense glassy phases of vortex matter [3]. On the other hand, relatively little is known about the dilute vortex phases under the combined influence of pinning centers and thermal fluctuations. A simulation by Gingras and Huse [8] has proposed that the addition of pinning can yield a reentrant glass phase at low densities (cf. Fig.1(b)), analogous to the low density vortex liquid phase (cf. Fig.1(a)) in an ideal pinning free situation.

A fruitful experimental investigation on different phases of vortex matter can come about via such experimentally accessible quantities, which are related to the extent of ordering of the vortices in the various phases. A theoretical framework which provides this link is the Larkin - Ovchinnikov (LO) description [9] propounded in the mid seventies. The LO theory showed that the extent of order maintained in the FLL in the presence of pinning can be quantified in terms of the radial (R_c) and the longitudinal (L_c) correlation lengths, which are distance scales over which the deviations \mathbf{u} of the flux lines from their mean periodic lattice positions become of the order of the radius of the core of the vortex, i.e., the coherence length ξ . The R_c and L_c , which are functions of the pinning strength and elastic moduli (which are functions of H and T), are inversely related to J_c as, $J_c \propto \frac{1}{\sqrt{R_c^2 L_c}}$. It is therefore possible to understand the changes in the behavior of J_c in terms of changes in R_c and L_c , which could happen due to occurrence of phase transformations in the vortex matter.

To enable us to study the evolution of the different phases of vortex matter under the combined influence of thermal fluctuations and quenched random inhomogeneities in the atomic lattice, we have used those experimental techniques (namely, ac susceptibility, dc magnetization measurements, transport experiments, etc.) which provide information on the behavior of J_c . A remarkable feature seen in the behavior of J_c in weakly pinned superconducting systems is the phenomenon of Peak Effect (PE) [2] prior to reaching the respective $H_{c2}(T)$ or $T_c(H)$. The pinning strength or J_c values usually decrease on increasing H or T . The PE relates to an anomalous increase in J_c , terminating in a peak, with increasing H (or T) while approaching H_{c2}/T_c . Despite many years of efforts, the PE still awaits complete theoretical understanding [10–12], however it is now widely accepted that PE signals the rapid softening of the elastic moduli of vortex solid and the occurrence of plastic deformation and proliferation of topological defects (like, dislocations) in FLL [12,13]. The vortex array is expected to be amorphous at and above the peak position in J_c [14]. The phenomenon of PE can therefore be exploited to gain information on different phases of vortex matter and the processes involved in enhancement of loss in order of FLL. We shall summarize in this paper the key experimental results of PE studies [15–21] in single crystals having progressively higher amounts of quenched pinning centers and belonging to an archetypal low T_c ($T_c(0) \sim 7$ K) weak pinning system 2H-NbSe₂. These results lead us to propose a generic phase diagram for a type II superconductor whose details make contacts with theoretical predictions summarized schematically in Fig.1(b). The proposed phase diagram finds support from identical behavior noted in a variety of other low T_c superconducting systems [16,22,23] and in a single crystal sample of a high T_c compound YBa₂Cu₃O₇ [24]. A glimpse into some of these results [22,23] shall also be provided here.

II. EXPERIMENTAL

The ac magnetic susceptibility, dc magnetization and dc resistivity studies have been performed using a standard mutual inductance bridge, a Quantum design SQUID magnetometer and the usual four probe method, respectively. The single crystal samples (A, B and C, with progressively increasing number of pinning centers) of hexagonal 2H-NbSe₂ system chosen for illustrating the results here belong to the same batches of crystals as utilized by different groups of experimentalists in recent years [25–27]. In each of these batches of crystals, the FLL with hexagonal arrangement is well formed at intermediate fields ($H > 0.5kOe$). The single crystals of some other superconducting systems such as *CeRu₂* ($T_c = 6.4$ K), *Ca₃Rh₄Sn₁₃* ($T_c = 8.5$ K), *YNi₂B₂C* ($T_c = 15.3$ K), etc. studied for comparison of trends emerging from data in 2H- NbSe₂ have levels of quenched random inhom-

geneities comparable to those in sample *C* of 2H-NbSe₂.

III. RESULTS AND DISCUSSIONS

A. Peak Effect Represents a Phase Transition

We shall first focus attention on an experimental result, which amounts to a compelling evidence in support of an assertion that PE peak qualifies for the status of a phase transition in vortex matter. Fig.2 depicts the typical variation in the real part of the ac susceptibility (χ') with temperature in nominal zero field and in an applied dc field of 4 kOe in the cleanest crystal *A* of 2H-NbSe₂ for $H_{dc}||c$. The χ' curve in zero field provides an estimate of the width $\Delta T_c(0)$ of the normal- superconducting transition. We will recall that when ac field has fully penetrated the superconducting sample, the χ' response can be approximated in Bean's critical state model as [28]:

$$\chi \sim -1 + \alpha \frac{h_{ac}}{J_c}; \quad \text{for } h_{ac} < H^*, \quad (1)$$

$$\chi \sim -\beta \frac{J_c}{h_{ac}}; \quad \text{for } h_{ac} > H^*, \quad (2)$$

where α and β are geometry and size dependent factors and H^* is the field at which screening currents flow throughout the sample. Note that initially at very low temperatures, $\chi' \approx -1$ (perfect shielding), when h_{ac} does not penetrate. However, as h_{ac} penetrates the sample, the temperature variation in χ' gets governed by the temperature variation in J_c . In zero field the diamagnetic χ' response monotonically increases (see Fig.2) due to an expected decrease in zero field current density $J_c(0)$ with the increase in temperature. However, in a dc field of 4 kOe, which creates a FLL with lattice constant $a_0 \approx 790\text{\AA}$, the usual decrease in diamagnetic $\chi'(T)$ response gets interrupted (cf. Fig.2) via a sudden onset (at $T = T_{pl}$) of an anomalous enhancement in the diamagnetic screening response; χ' reaches a sharp minimum at $T = T_p$, above which χ' recovers rapidly towards the normal state value at $T_c(H)$. Note that the rate of rapid recovery of the latter is very much higher than the rate at which the diamagnetic χ' response was decreasing prior to the onset of anomalous dip in χ' at $T = T_{pl}$. The non-monotonicity in χ' is a consequence of non-monotonicity in $J_c(H, T)$ such that the minimum in χ' corresponds to a peak in J_c , the ubiquitous peak effect (PE). The experimental fact is that the width of the PE region is decisively smaller than the width of superconducting transition ($\Delta T_c(0)$) in zero field (cf. Fig.2). It may be further noted (see the inset of Fig. 2) that J_c crashes towards a zero value from peak position of PE such that the diamagnetic χ' response transforms to a paramagnetic response across the so called irreversibility temperature, T_{irr} . Above T_{irr} , $J_c \approx 0$ and the mixed state of the superconductor is in its reversible phase, whose differential magnetic

response is positive (i.e., diamagnetic dc magnetization decreases as dc field/temperature increases). The differential paramagnetic effect (DPE) region in the inset of Fig.2, therefore, identifies the depinned ($J_c=0$) state of vortex matter in between irreversibility temperature $T_{irr}(H)$ and the superconducting temperature $T_c(H)$. To summarize, in a $\chi'(T)$ measurement at a fixed H , we can in principle identify four temperatures denoted as T_{pl} , T_p , T_{irr} and T_c . In the subsequent sections, we will present more experimental results which elucidate and characterize the different phases of vortex matter corresponding to $T < T_{pl}$, $T_{pl} < T < T_p$ and $T_p < T < T_{irr}$.

In weakly pinned systems, J_c is given by the pinning force equation:

$$J_c B = \left(\frac{n_p \langle f_p^2 \rangle}{V_c} \right)^{\frac{1}{2}} = \left(\frac{n_p \langle f_p^2 \rangle}{R_c^2 L_c} \right)^{\frac{1}{2}}, \quad (3)$$

where n_p is the density of pins, f_p is the elementary pinning interaction proportional to the condensation energy and V_c is the correlation volume of a Larkin domain, within which flux lines retain their nominal hexagonal symmetry. As per eqn.(3.3), the PE in J_c corresponds to a rapid shrinkage in V_c (more rapid than the decrease in $\langle f_p^2 \rangle$, which causes the usual monotonic decrease in ac screening response with increase in T or H), so as to produce an overall enhancement in J_c upto the peak position of PE. Above the peak position, the rapid collapse in χ' is expected to be governed entirely by a sharp change in elementary pinning interaction f_p while approaching the superconductor to normal boundary. Transport [13] and noise studies [29] on driven vortex matter in very clean crystals of 2H- NbSe₂ have earlier provided indications that the underlying depinned lattice (in the absence of external driving force) between the onset and peak positions of PE is probably in plastically deformed state in contrast to an elastically deformed vortex state existing prior to the onset of PE. We shall provide evidences here in favor of the scenario that the role of plastic deformations (and consequently that of shrinkage in V_c) ceases at the peak position of PE. It will also be elucidated that the onset of shrinkage in V_c is induced by the pinning effects in a characteristically novel manner.

B. Structure in Peak Effect and Identification and Characterization of Phase Transformations

Fig.3 collates the plots of loci of four features, the onset of PE at H_{pl} , T_{pl} , the location of peak of PE at H_p , T_p , an apparent irreversibility line (H_{irr}, T_{irr}) and the superconducting-normal phase line (H_{c2}, T_c), in crystals *A*, *B* and *C* of 2H- NbSe₂ for fields larger than 1 kOe (i.e., for vortex arrays with lattice constants $a_0 < 1600\text{\AA}$). Note that the anomalous PE region spanning from (H_{pl}, T_{pl}) to (H_{irr}, T_{irr}) through (H_p, T_p) in extremely weakly pinned cleanest sample *A* is so narrow

that it suffices for us to identify only its H_p line whose thickness encompasses its (H_{pl}, T_{pl}) and (H_{irr}, T_{irr}) data points as well. The PE region can be seen to become a little broader in weakly pinned crystal B such that the H_{pl} , H_p and H_{irr} lines in it can be distinctly drawn in Fig. 3. However, as the pinning increases and one moves onto the nominally weakly pinned sample C, the PE region can be seen to expand over considerably larger region of (H, T) phase space. It can be noted in Fig.3 that the H_{pl} line moves away from H_{irr} line as H increases. The separation between the H_{pl} and H_p lines also correspondingly increases even though H_p line remains relatively more close to the H_{irr} line. In the vortex phase diagram of sample C, we have labeled the region below the H_{pl} line as the *elastic glass* and that between the H_{pl} and H_p lines as the *plastic glass*. The regions above the H_p line have been given the names *pinned amorphous* (for $H_p < H < H_{irr}$) and *unpinned amorphous* (for $H_{irr} < H < H_{c2}$), respectively.

As a step towards rational explanation of these nomenclatures, we focus attention onto $\chi'(T)$ behavior (see Figs.4(a) and 4(b)) in sample C in a field of 5 kOe ($a_0 \approx 700\text{\AA}$). In Fig.4(a), we show a comparison of $\chi'(T)$ response in vortex states obtained at low temperatures ($T \ll T_c$) via two entirely different thermomagnetic histories, namely, zero field cooled (ZFC) and field cooled (FC). Note that in the ZFC case, $\chi'(T)$ behavior displays a well recognizable PE peak. On the other hand, the same feature is far less conspicuous in the data recorded during the field cooled warm up (FCW) mode. Prior to the peak position of PE, χ' response in the FC state is more diamagnetic than that in the ZFC state and above the peak temperature T_p , the difference between the two responses dramatically disappears (*a la spin glass phenomenon*). The observed behavior is usually understood in terms of history dependence in the values of J_c (cf. eqn.1), such that $J_c^{FC} > J_c^{ZFC}$ for $T < T_p$ [16,20]. Eqn.2 implies that history dependence in J_c reflects the history dependence in correlation volume V_c , as neither n_p nor f_p , both microscopic quantities for the same realization of quenched random disorder, can depend on the thermomagnetic history of the vortex system. We have argued earlier [16] that in a given circumstance, V_c attains the minimum value at the peak position of PE. The observation that the diamagnetic χ' in FC state at $T \ll T_p$ is not very different from its value at $T = T_p$ implies that the correlation volume V_c at $T \ll T_p$ is the *supercooled* state existing at the peak position of PE. Thus, in the ZFC state, the correlation volume of the vortex state prior to the arrival of the PE region ($T \ll T_p$) is much larger than that in the FC state. It can, therefore, be concluded that the ZFC vortex state is a well ordered one and the FC state at low temperatures attempts to freeze in the maximally disordered (i.e., the amorphous phase) existing at $T \approx T_p$. Note, further, that $\chi'(T)$ of the ZFC state shows two sharp ($< 1mK$ in width) jumps at $T \approx T_{pl}$ and at $T \approx T_p$. These jumps amount to sudden shrinkages in the V_c near the onset and peak

positions of PE.

The sharp changes in V_c are candidates for first order like phase transitions in vortex matter under the combined influence of thermal fluctuations and pinning centers. To fortify this assertion, we elucidate here the occurrence of irreversible behavior while thermal cyclings across both the temperatures T_{pl} and T_p . We show in Fig.4(b) the $\chi'(T)$ data obtained in sample C in a field of 5 kOe while cooling down from temperatures T_I , T_{II} and T_{III} lying in three different regions, viz., (i) $T_I < T_{pl}$, (ii) $T_{pl} < T_{II} < T_p$ and (iii) $T_p < T_{III} < T_{irr}$. The $\chi'(T)$ data recorded during warm up of ZFC and FC states are indicated by a dotted curve and a solid curve (data points omitted), respectively in Fig.4(b). From this figure, it is apparent that while cooling down from T_I , $\chi'(T)$ response retraces its path (i.e., the dotted ZFC curve). However, while cooling down from T_{II} , the $\chi'(T)$ response (see filled circle data points) attempts to retrace its path while approaching T_{pl} , but as it nears the temperature T_{pl} , the $\chi'(T)$ response suffers a sharp fall to a diamagnetic value which lies closer to that of the completely amorphous FC like state. On cooling down further below T_{pl} , the χ' response never recovers on its own towards the $\chi'(T)$ response of the ordered ZFC like state. This striking result can be rationalized in terms of the following scenario. When an ordered ZFC like state is warmed up towards the PE region, the FLL softens, the energy needed to create dislocations decreases and the lattice spontaneously (partially) fractures at T_{pl} . Upon lowering the temperature from within the PE region ($T_{pl} < T < T_p$), the lattice stiffens and the stresses build up. The partially disordered vortex system fails to drive out dislocations in order to heal back to an ordered ZFC like state. Instead, it shatters further to relieve its stresses and reaches the completely amorphous FC like metastable state. This yields an open hysteresis curve in T , i.e., one cannot recover the original ordered state by cycling in temperature alone. This is a novel feature, not seen in the usual first order transitions in which only the thermal fluctuations are involved. There are compelling evidences that this feature is controlled by effective pinning in the system. In Fig.4(b), it can finally be noted that while cooling down from a temperature T_{III} lying above T_p , $\chi'(T)$ response (see the solid triangle data points) faithfully retraces its path while approaching T_p . Below T_p , the cool down $\chi'(T)$ response starts to differ from that recorded earlier during warm up cycles for ZFC and FCW states in the same temperature interval. It is clear that $d\chi'/dT$ is negative between T_{pl} and T_p during warm up cycle (cf. dotted curve in Fig.4(b)), whereas it is positive for cool down from T_{III} in the same temperature interval. Note, also, that eventually at $T < T_{pl}$, i.e., after a jump in $\chi'(T)$ happens while cool down from T_{II} , the $\chi'(T)$ response of both the cool down cycles not only nearly overlap but they are also not very different from the $\chi'(T)$ response recorded during FCW cycle. The data of Fig.4(b) thus clearly indicate that the transformation occurring in the vortex matter near the peak tempera-

ture T_p is such that the past history of the vortex state is immaterial for its behavior above T_p . It can therefore be surmised that the vortex state is disordered in equilibrium at $T > T_p$ and the state of disorder existing at $T \approx T_p$ can be preserved or supercooled down to much lower temperatures (i.e., $T \ll T_p$). In between T_{pl} and T_p , the ordered state formed via ZFC (at $T \ll T_{pl}$) mode gets shattered in a stepwise manner.

The onset and peak positions have special significance in the sense that cyclings across them produce the unusual open hysteresis curves in T. We have demonstrated [15] recently that the first sharp jump in χ' near the onset position is a special attribute of the disordering process of FLL which is induced by pinning centers as they take advantage of the incipient softening of the lattice at PE. The connection between the history dependence or metastability in vortex lattice can be appreciated by examining the $\chi'(T)$ data recorded in ZFC and FCW modes at the same field (fixed inter-vortex spacing a_0) in samples with differing quenched inhomogeneities (like samples A, B and C of $NbSe_2$) or at different fields (i.e., by changing the inter-vortex spacing a_0) in a given sample. It has often been argued [30] that an increase in field (i.e., decrease in a_0) amounts to an increase in effective pinning as the pinning induced wanderings of the flux lines from their mean positions do not decrease with field in the same proportion as the decrease in a_0 with field. Thus, the ratio $\Delta a_0/a_0$ (where Δa_0 is the pinning induced spread in a_0), which can be taken as a measure of the effective pinning, increases as H increases. We have shown earlier [15] how the first jump in χ' and the associated structure and metastability effects in χ' response between T_{pl} and T_p are intimately related. The first jump in χ' can be suppressed and the details of structure in χ' between T_{pl} and T_p can be compromised under various circumstances [31], however, the feature of negative peak in χ' at T_p is robust. For instance, the vortex state prior to the arrival of PE region can be reorganized to a state of even better order (than that in the nominal ZFC mode) by subjecting the lattice to a sizable driving force via the process of cyclings in large enough ac fields. In such circumstance, the behavior of the kind (in ZFC mode) shown in Fig. 4(a) could transform to that shown in Fig.2, i.e., the first jump in χ' near T_{pl} could be made to disappear, and the detailed structure in χ' smoothed out.

A qualitative feature that emerges from the high field χ' data in different crystals of 2H-NbSe₂ can be summarized as follows. A well correlated (pinned) FLL state loses order in a stepwise manner based on the competition among three energy scales: the elastic energy E_{el} , the pinning energy E_{pin} and thermal energy E_{th} . At low T, E_{el} dominates and a phase akin to an elastic (Bragg) glass occurs. With increasing T, E_{el} decreases faster than E_{pin} , and above the (H_{pl}, T_{pl}) line, E_{pin} dominates, leading to proliferation of topological defects, likely similar to a vortex glass-entangled solid phase. At even higher tem-

peratures at the (H_p, T_p) line, the E_{th} overcomes E_{el} , and the residual disorder is presumably lost due to thermal fluctuation effects (or the effects arising out of setting in of divergence in values of intrinsic parameters, like, λ and ξ near superconductor-normal phase boundary). The disordered state between (H_p, T_p) and (H_{irr}, T_{irr}) is pinned with $J_c \neq 0$. Finally, a dynamical crossover to unpinned region ($J_c \approx 0$) occurs above the (H_{irr}, T_{irr}) line and the (H_{c2}, T_c) line identifies the boundary where the diamagnetic response in dc magnetization measurements falls below a measurable limit.

C. Reentrant Characteristic in Peak Effect Curve and the Effect of Pinning on it

There is a widespread consensus that the PE curve (H_p, T_p) separates the ordered and disordered phases of vortex matter. Direct structural support for this view point is now also growing via diffraction data obtained from small angle neutron scattering experiments and via microscopic muon spin rotation studies on a variety of different superconducting systems, such as, pure Nb [14], NbSe₂ [32], (K,Ba)BiO₃ [33], etc.. Keeping these in view, we recall that Ghosh *et al* [27] had shown that $T_p(H)$ curve determined from $\chi'(T)$ at low fields (< 2 kOe) in sample B of 2H-NbSe₂ displayed a reentrant characteristic, which bore striking resemblance to the theoretically proposed re-entrant melting phase boundary shown in the schematic phase diagram of Fig.1(a). The turnaround (or the reentrance) in $T_p(H)$ curve in sample B of 2H-NbSe₂ has been reported [34] for H||c and H||ab at $H \sim 100$ Oe, where FLL constant a_0 exceeds the range of interaction (i.e., the penetration depth values) of vortex lines. The turnaround in $T_p(H)$ is accompanied by rapid broadening and eventual disappearance of PE peak both in magnetic as well as transport studies [17], and such a behavior is rationalized by stating that as the inter-vortex interaction effects weaken, the collectively pinned elastic vortex solid makes a crossover to the small bundle or individual pinning regime, which is once again dominated by pinning effects of quenched random inhomogeneities. The reentrant characteristic in $T_p(H)$ curve therefore, also, implies that as the field gets varied at a fixed temperature (isothermal scan), one should first encounter the pinning dominated disordered dilute vortex state (where $a_0 > \lambda$). This should be followed by interaction dominated well ordered phase, which should eventually once again transform to a disordered (amorphous) phase at very high vortex densities ($\lambda \gg a_0 \leq \xi$).

A careful examination of the phase diagram shown in Fig.3 reveals that for a fixed value of reduced temperature t , the onset line (H_{pl}, T_{pl}) of PE progressively moves inwards from sample A to sample C. This means that the phase space of ordered elastic solid shrinks along the upper portion of the PE curve as the pinning effects increase. If the same notion is to hold for the lower

(reentrant) portion of the PE boundary determined first by Ghosh *et al* [27], the reentrant leg of the PE curve should move upwards as pinning effects increase. This indeed is the experimental situation [17]. Fig.5 collates the plots of $t_p(H)$ curves in samples A, B and C in the low field region ($H < 1$ kOe). For the purpose of reference, the $H_{c2}(t)$ curve has also been drawn for sample A in Fig.5 and it may be assumed that $H_{c2}(t)$ curves for other two samples overlap with that of sample A. Note first the error bars on the data points of samples B and C as the dc field decreases below 500 Oe. In sample C, the PE broadens so much that the PE peak cannot be distinctly identified below about 200 Oe [17]. In sample A, however, a sharp PE peak (as in Fig.2) can be distinctly seen in $\chi'(T)$ scans in fields as low as 30 Oe. The $t_p(H)$ curve in sample A has a turnaround feature but its lower (reentrant leg) portion could not be determined from temperature dependent scans of the in-phase ac susceptibility data. However, the trend that the reentrant lower leg of $t_p(H)$ curve should move upwards, as the pinning effects progressively enhance from sample A to C, stands satisfactorily demonstrated.

D. Evolution in Pinning Behavior and Identification of Reentrant Disordered Region for Dilute Vortex Arrays

In order to more convincingly elucidate the reentrant characteristic in order to disorder transformation (cf. schematics drawn in Fig.1(b)) as the field is increased in an isothermal scan, we focus attention onto Figs.6(a) to 6(d) and Figs.6(e) to 6(h). These data [21] on current densities were extracted from an analysis of isothermal in-phase and out-of-phase ac susceptibility data as per a prescription of Angurel *et al* [35] and the estimates were verified via dc magnetization hysteresis measurements.

Figs.6(a) to 6(d) show $J_c(H)$ vs H on log-log plots in sample B for four reduced temperatures as identified by open circle data points lying on $t_p(H)$ curve included in the inset of Fig.6(c). Similarly, Figs.6(e) to 6(h) depict data in sample A for four temperature values marked in the inset of Fig.6(g). The two sets of plots elucidate the generic nature of evolution in shapes of $J_c(H)$ vs H behavior. We first focus on pairs of plots in Figs.6(a) and 6(d) and in Figs.6(e) and 6(h). In both the Figs.6(a) and 6(e), we can identify three regimes, marked I, II and III in each of them. The regime III identifies the quintessential peak effect phenomenon. The field region II, in which $J_c(H)$ decays with H in a power law manner ($J_c \sim H^{-1}$) identifies the collectively pinned elastic vortex solid. The low field region I identifies the field span in which the vortices are in a small bundle or individual pinning regime and consequently $J_c(H)$ decays more weakly with H as compared to the decay rate seen in the power law regime II. Note that the power law region II extends down to much lower field values (~ 10 Oe) in sample A as compared to that (~ 200

Oe) in sample B. In fact in sample B, the $J_c(H)$ values move towards the saturation $J_c(H=0)$ limit of regime I in a faster manner than the extrapolated dotted line (of power law regime) desires in Fig.6(a). This faster approach to the saturated amorphous limit (see Figs.7(a) and 7(b) for a replot of the data in Figs.6(a) to 6(h) in a normalized manner) is in fact the low field counterpart of the approach to the peak value of $J_c(H)$ at the peak position of PE at high fields. Now, we turn to the behavior shown in Figs.6(d) and 6(h), where $J_c(H)$ decays very slowly and monotonically with H (upto the highest field values) and the PE region cannot be distinctly identified. Note that the (reduced) temperatures corresponding to Figs.6(d) and 6(h) in samples B and A, respectively, are located near the turnaround portion of their respective $t_p(H)$ curves in the insets of Figs.6(c) and 6(g). In an isothermal scan at such a temperature, the well ordered collectively pinned regime is not expected to be encountered. The low field small bundle pinning regime is expected to crossover to the higher field amorphous vortex phase in a contiguous manner. The plots in Figs.6(b) and 6(c) and in Figs.6(f) and 6(g) elucidate how the collectively pinned well ordered region sandwiched (see arrow marks in each figure) between the disordered states shrinks as the temperature increases while approaching the limiting value corresponding to the turnaround point of respective $t_p(H)$ curves.

We collate all the data shown in Fig.6 in two sets of normalized plots for samples A and B in Figs.7(a) and 7(b), respectively. The evolution in shapes of current density vs reduced field ($H/H_{c2}(T)$) curves in the two sets of plots is remarkably similar to the evolution in behavior reported earlier in weakly pinned single crystals of an archetypal low T_c alloy superconductor V_3Si [36,37] and an archetypal high T_c cuprate superconductor $YBa_2Cu_3O_7$ [37,38]. This fact attests to the generic nature of the observed behavior across different classes of superconductors. The electromagnetic response of type-II materials and the details of the vortex phase diagrams in them appear to bear little relationship with the microscopics of the different varieties of superconducting systems.

The plots in Figs.7(a) and 7(b) clearly bring out how the PE broadens as the effects due to interplay between the thermal fluctuations and the pinning effects enhance while approaching the turnaround feature in a PE curve. It can be noted that when the PE is very pronounced, $J_c(H)$ rises from its smallest value at the end of collectively pinned power law regime (i.e., at the onset of PE) to reach its overall amorphous limit at the peak position (see curves from $t=0.973$ to 0.990 in Fig.7(a) and those from $t=0.965$ to 0.973 in Fig.7(b)). At the lower field end of the power law regime as well, the $J_c(H)$ starts to rise faster on lowering the field further (see the curve for $t=0.965$ in Fig.7(b)) and reaches the small bundle pinning limit. From the high field amorphous limit, $J_c(H)$ can only decrease on increasing the field towards H_{c2} (i.e., $b=1$) and, thereby, it yields a peak effect phenomenon in

$J_c(H)$. On the otherhand, at the lowest field once the small bundle pinning limit is attained, the $J_c(H)$ values can flatten out towards the $J_c(0)$ value. This inevitable happening has prompted us recently [21] to propose that the said feature be better designated as the *Plateau Effect* instead of *reentrant peak effect*, as described earlier [17]. Finally, a careful examination of the shapes of the curves at $t=0.983$ and 0.99 in Fig.7(a) and that at $t=0.977$ in Fig.7(b) reminds us of the phenomenon of second magnetization peak or the so called *fishtail* anomaly widely reported in the context of high T_c cuprates in recent years [37,38]. It may be useful to mention here that the *fishtail* effect relates to a characteristic shape of the isothermal dc magnetization hysteresis loop. The display of data in Figs.7(a) and 7(b), therefore, provides a natural understanding of the fishtail type anomalous behavior in $J_c(H)$ in the context of the presence of the plateau effect for dilute vortex arrays at low fields and the usual peak effect for dense vortex arrays at high fields.

We present in Figs.8(a), 8(b) and 8(c) the vortex phase diagrams in samples A, B and C, respectively at the low fields and high temperatures (close to $T_c(0)$). These phase diagrams have been determined from the identification of regimes I, II and III via plots as in Fig.6. The lower ends of collectively pinned regime II at different temperatures have been marked by filled triangle data points, whereas, the upper ends of regime II coincide with the dotted curve $H_{pl}(t)$, which identifies the onset position of PE. The span of regime I, named as the reentrant disordered (following schematics in Fig.1(b)) in Figs.8(a) to 8(c), can be identified by slanted lines. The regime III corresponding to the PE phenomenon has been termed as amorphous (see the regions spanned by dotted lines) in both the phase diagrams. The so called reentrant disordered and amorphous regions overlap and form a continuum near the turnaround point of the H_{pl} curve. Above the temperature corresponding to the turnaround point, the vortex matter remains in a disordered state at all fields presumably due to juxtaposition of effects due to thermal fluctuations and pinning. However, at temperatures sufficiently below the turnaround temperature, one would find the collectively pinned FLL sandwiched between an individually pinned disordered low density phase and the plastically deformed (partially amorphous) high density phase. It is apparent that the (H,T) phase space corresponding to the collectively pinned ordered state progressively shrinks as one goes from the cleanest sample A to the nominally pure sample C, however the reentrant characteristic in disorder to order transformation phenomenon stands elucidated in all the three samples.

E. Vortex Phase Diagrams in Other Low T_c Systems

In earlier sections, we described results pertaining to the construction of vortex phase diagrams in weakly

pinned samples of 2H-NbSe₂, which has emerged as the most favored superconducting system for vortex state studies for its optimum values [13] of Ginzburg number G_i and the ratio J_c/J_0 , where J_0 is the depairing current density. However, in recent years, many reports on the construction of vortex phase diagrams have appeared in wide classes of other low T_c superconducting systems, such as, heavy fermion superconductors, UPd₂Al₃, UPt₃, etc., [39] mixed valent rare earth intermetallics, such as CeRu₂ [16], Yb₃Rh₄Sn₁₃ [40,41], etc., ternary stannides, like Ca₃Rh₄Sn₁₃ [42], quaternary borocarbide [43] superconductors, such as, YNi₂B₂C, etc. It has often been stated that some of the phase boundaries (locus of H and T values) drawn for all these systems extend over similar parametric limits in the normalized (H,T) phase space. Some reports [44] have also drawn attention to the similarities in the characteristics (in transport studies) of different vortex phases identified in systems, like CeRu₂, YBa₂Cu₃O₇, and 2H- NbSe₂. In a recent study, some of us have shown that the vortex phase diagram in a weakly pinned single crystal of CeRu₂ is nearly identical to that in sample C of 2H-NbSe₂ [16]. It is our assertion that the weakly pinned samples of most other superconducting systems also display detailed behavior in the PE region similar to that observed in sample C. In isofield ac susceptibility studies, the PE region comprises two first order like jumps at the onset and the peak positions of PE. In between these two jumps, χ' often displays a two peak like structure [15,16]. Our ansatz is that the first peak reflects the commencement of pinning induced stepwise shattering of FLL through sudden shrinkage of correlation volume V_c at T_{pl} due to proliferation of dislocations. The disappearance of history dependence above T_p reflects the absence of memory of previous history and the complete amorphisation of FLL. We present in Figs.9(a) and 9(b) the $\chi'(T)$ data at fixed fields in single crystals of two more superconducting systems, namely, Ca₃Rh₄Sn₁₃ [22] and YNi₂B₂C [23] in support of the above ansatz. In both these figures, the onset (T_{pl}) and peak (T_p) positions of PE phenomenon have been marked. Collection of such data along with the measurements of isothermal magnetization hysteresis loops lead us to the construction of vortex phase diagrams in Ca₃Rh₄Sn₁₃ and YNi₂B₂C shown in Figs.10(a) and 10(b), respectively. The similarity between these phase diagrams and that shown for sample C in Fig.3 amply justify the assertion made above. The PE phenomenon cannot be observed in crystals of Ca₃Rh₄Sn₁₃ and YNi₂B₂C in fields below few kOe, where FLL constant a_0 ($\sim 1000 \text{ \AA}$) exceeds the respective penetration depth values and the pinning effects dominate over interaction effects. This accounts for the termination of H_{pl} and H_p lines at low field ends as shown in the Figs.10 (a) and (b).

IV. CONCLUSION

The advent of the phenomenon of high temperature superconductivity stimulated search for different possible phases (and transformations among them) of vortex matter formed as a consequence of competition amongst interaction between the vortices and the disorder effects caused by thermal fluctuations and inevitable presence of quenched random inhomogeneities in the underlying atomic lattice. Theoretical studies [3–8] during the last decade have brought out how different phases of vortex matter could be distinguished on the basis of the characteristics of spatial and temporal correlations amongst vortices. The phase boundary separating the (quasi) Abrikosov flux line lattice and the quasi-vortex liquid phases has received the most extensive attention from the experimentalists. In the field-temperature regions, where thermal fluctuation effects dominate over pinning disorder in the context of high T_c cuprate systems, magnetic, thermal and structural studies have elucidated that the ordered vortex solid to the (disordered) vortex liquid transition is first order in character [45–49]. A crucial evidence in favor of this inference has been an observation of a step increase in equilibrium magnetization (ΔM_{eq}) via bulk and local magnetization measurements [45,46,48], which translates into a change in entropy (ΔS) and the latent heat L via the Clausius-Clapeyron relation; $L = T\Delta S = -T(\Delta M_{eq})(\delta H_m/\delta T)$. In weakly pinned samples of low T_c superconductors, our assertions about the different phases of vortex matter and the transformations amongst them have been based on the characteristic details of the peak effect and their relationships to the order to disorder phenomenon. The change in equilibrium magnetization that could be related to order-disorder transition across the PE is difficult to discern experimentally as the PE itself manifests as an anomalous increase in irreversible magnetization [18]. However, in a limited field-temperature region of a very clean crystal of 2H-NbSe₂, Ravikumar *et al* [20] have revealed the presence of ΔM_{eq} across the PE. The estimated entropy change associated with order-disorder transition across PE is of the same order as observed earlier in the context of melting of FLL in cuprate compounds [20,48,49]. Direct structural studies [14,33] across PE in weakly pinned samples of low T_c superconductors support the notion of occurrence of a transformation from an ordered (quasi FLL) vortex solid to an amorphous vortex phase. Furthermore, muon spin mutation studies at low fields in crystals of 2H-NbSe₂ have revealed the occurrence of a change in state of vortex matter across PE which is no different from the changes reported in the context of the fishtail effect and the melting of FLL in similar studies in cuprate superconductors [32,50].

In view of the above, we are tempted to propose a generic phase diagram for a realistic sample of a type-II superconductor which is weakly pinned. We show a schematic view of such a phase diagram in Fig.11, which

has been drawn on the basis of experimental data in sample *B* of 2H-NbSe₂. The generic phase diagram comprises six phases, viz., an elastically deformed vortex solid phase akin to a Bragg glass ($H < H_{pl}$), a plastically deformed vortex glass phase ($H_{pl} < H < H_p$), a pinned ($J_c \neq 0$) amorphous phase ($H_p < H < H_{irr}$) and an unpinned ($J_c \approx 0$) amorphous phase ($H_{irr} < H < H_{c2}$), a low density reentrant glass phase ($H_{c1} < H < H_{low}$) and a Meissner phase ($H < H_{c1}$). The (dotted) boundary separating the reentrant glass and the Bragg glass phases represents a crossover phenomenon. The vortex matter above the PE boundary (H_p) is disordered in inequilibrium in the sense that no metastability effects are observed above this boundary. However, the vortex matter can be obtained in a disordered metastable state below the H_p line by the process of field cooling, which is analogous to the phenomenon of supercooling below a first order transition. An application of driving force can reorganize the disordered metastable state towards an ordered stable state [51]. Recent experiments [52] have revealed that between the H_{pl} and H_p lines, the stationary state of the vortex matter is a partially ordered state. In such a region, the vortex matter can be obtained in a *metastable* well ordered state or a *metastable* amorphous state by the process of superheating or supercooling, respectively. An application of a driving force could transform both types of metastable configurations to the stable partially ordered state.

A phenomenological understanding of transformations between the metastable and stable phases of vortex matter has also been achieved recently via the proposition of a new model [53] which reduces to the well known critical state model due to C. P. Bean [54] in the absence of metastability effects. We thus believe that the task of sketching a magnetic phase diagram of conventional type-II superconductors stands accomplished [55] fairly satisfactorily both from experimental view point as well as phenomenological (theoretical) considerations. Many interesting details, however, need to be precisely investigated as well as quantitatively accounted for.

V. ACKNOWLEDGEMENT

This review is primarily based on the experiments performed at Mumbai, India in association with our collaborators internationally, who provided us the high quality single crystals of a variety of superconducting compounds. In particular, we would like to acknowledge our cooperation with the groups of Prof. Y. Onuki (Osaka, Japan), Prof. D. Mck Paul (Warwick, U.K.) and Dr. H. Takeya (Tsukuba, Japan) and Dr. P. Gammel (Lucent Technologies, Murray Hill, U.S.A.).

Corresponding authors :
ramky@tifr.res.in/grover@tifr.res.in

-
- [1] A. A. Abrikosov, Sov. Phys. JETP **5** (1957) 1174.
- [2] Michael Tinkham, Introduction to Superconductivity, Mc Graw-Hill, Inc. U.S.A., Second edition (1996).
- [3] G. Blatter, M. V. Feigel'man, V. B. Geshkenbein, A. I. Larkin and V. M. Vinokur, Rev. Mod. Phys. **66** (1994) 1125 and references cited therein.
- [4] D. R. Nelson, Phys. Rev. Lett. **60** (1988) 1973.
- [5] D. S. Fisher, M. P. A. Fisher and D. A. Huse, Phys. Rev. B **43** (1991) 130.
- [6] T. Giamarchi and P. Le Doussal, Phys. Rev. Lett. **72** (1994) 1530.
- [7] T. Giamarchi and P. Le Doussal, Phys. Rev. B **52** (1995) 1242 and references therein.
- [8] M. J. P. Gingras and D. A. Huse, Phys. Rev. B **53** (1996) 15193.
- [9] A. I. Larkin and Yu. N. Ovchinnikov, Sov. Phys. JETP **38** (1974)854.
- [10] A. I. Larkin and Yu. N. Ovchinnikov, J. Low Temp. Phys. **34** (1979) 409.
- [11] A. I. Larkin, M. C. Marchetti and V. M. Vinokur, Phys. Rev. Lett. **75** (1995) 2992.
- [12] C. Tang, X. S. Ling, S. Bhattacharya and P. M. Chaikin, Europhys. Lett. **35** (1996) 597.
- [13] M. J. Higgins and S. Bhattacharya, Physica C **257** (1996) 232 and references cited therein.
- [14] P. L. Gammel, U. Yaron, A. P. Ramirez, D. J. Bishop, A. M. Chang, R. Ruel, L. N. Pfeiffer and E. Bucher, Phys. Rev. Lett. **80** (1998) 833.
- [15] S. S. Banerjee, N. G. Patil, S. Ramakrishnan, A. K. Grover, S. Bhattacharya, G. Ravikumar, P. K. Mishra, T. V. Chandrasekhar Rao, V. C. Sahni, M. J. Higgins, C. V. Tomy, G. Balakrishnan and D. Mck Paul, Phys. Rev. B, **59** (1999) 6043.
- [16] S. S. Banerjee, N. G. Patil, S. Saha, S. Ramakrishnan, A. K. Grover, S. Bhattacharya, G. Ravikumar, P. K. Mishra, T. V. Chandrasekhar Rao, V. C. Sahni, M. J. Higgins, E. Yamamoto, Y. Haga, M. Hedo, Y. Inada and Y. Onuki, Phys. Rev. B **58** (1998) 995.
- [17] S. S. Banerjee, N. G. Patil, S. Ramakrishnan, A. K. Grover, S. Bhattacharya, G. Ravikumar, P. K. Mishra, T. V. Chandrasekhar Rao, V. C. Sahni, M. J. Higgins, C. V. Tomy, G. Balakrishnan and D. Mck Paul, Euro. Phys. Lett. **44** (1998) 91.
- [18] G. Ravikumar, T. V. C. Rao, P. K. Mishra, V. C. Sahni, Subir Saha, S. S. Banerjee, N. G. Patil, A. K. Grover, S. Ramakrishnan, S. Bhattacharya, E. Yamamoto, Y. Haga, M. Hedo, Y. Inada and Y. Onuki, Physica C **276** (1997) 9.
- [19] G. Ravikumar, P. K. Mishra, V. C. Sahni, S. S. Banerjee, A. K. Grover, S. Ramakrishnan, P. L. Gammel, D. J. Bishop, E. Bucher, M. J. Higgins and S. Bhattacharya, (submitted to Phys. Rev. B); <http://xxx.lanl.gov/abs/cond-mat/9908222>.
- [20] G. Ravikumar, P. K. Mishra, V. C. Sahni, S. S. Banerjee, S. Ramakrishnan, A. K. Grover, P. L. Gammel, D. J. Bishop, E. Bucher, M. J. Higgins and S. Bhattacharya, Physica C (in press).
- [21] S. S. Banerjee, S. Ramakrishnan, A. K. Grover, G. Ravikumar, P. K. Mishra, V. C. Sahni, C. V. Tomy, G. Balakrishnan, D. Mck. Paul, P. L. Gammel, D. J. Bishop, E. Bucher, M. J. Higgins and S. Bhattacharya, (submitted to Phys. Rev. B); <http://xxx.lanl.gov/abs/cond-mat/9907111>.
- [22] Shampa Sarkar, D. Pal, S. S. Banerjee, S. Ramakrishnan, A. K. Grover, C. V. Tomy, G. Ravikumar, P. K. Mishra, V. C. Sahni, G. Balakrishnan, D. Mck. Paul and S. Bhattacharya, (submitted to Phys. Rev. B) ; <http://xxx.lanl.gov/abs/cond-mat/9909297>.
- [23] D. Pal, Shampa Sarkar, S. S. Banerjee, S. Ramakrishnan, A.K.Grover, S. Bhattacharya, G. Ravikumar, P. K. Mishra, T.V.C. Rao, V. C. Sahni and H. Takeya, *Proceedings of the DAE Solid State Physics Symposium*, **40C** (1997) 310.
- [24] D. Pal, D. Dasgupta, B. K. Sarma, *et al*, (unpublished).
- [25] S. Bhattacharya and M. J. Higgins, Phys. Rev. Lett. **70** (1993) 2617.
- [26] W. Henderson, E. Y. Anderi, M. J. Higgins and S. Bhattacharya, Phys. Rev. Lett. **77** (1996) 2077.
- [27] K. Ghosh, S. Ramakrishnan, A. K. Grover, Gautam I. Menon, Girish Chandra, T. V. Chandrasekhar Rao, G. Ravikumar, P. K. Mishra, V. C. Sahni, C. V. Tomy, G. Balakrishnan, D. Mck Paul and S. Bhattacharya, Phys. Rev. Lett., **76** (1996) 4600.
- [28] X. S. Ling and J. Budnick, in Magnetic Susceptibility of Superconductors and other Spin Systems, edited by R. A. Hein, T. L. Francavilla, and D. H. Leibenberg (Plenum Press, New York, 1991), p. 377.
- [29] R. Merithew, M. W. Rabin and M. B. Weismann, M. J. Higgins and S. Bhattacharya, Phys. Rev. Lett. **77** (1996) 3197.
- [30] G. I. Menon and C. Dasgupta, Phys. Rev. Lett. **73** (1994) 1023.
- [31] S. S. Banerjee, Ph. D. thesis, 1999. University of Mumbai, Mumbai, India.
- [32] T. V. C. Rao, V. C. Sahni, P. K. Mishra, G. Ravikumar, C. V. Tomy, G. Balakrishnan, D. Mck Paul, C. A. Scott, S. S. Banerjee, N. G. Patil, S. Saha, S. Ramakrishnan, A. K. Grover, S. Bhattacharya, Physica C **299**(1998) 267.
- [33] I. Journaud, J. Marcus, T. Klein and R. Cubitt, Phys. Rev. Lett. **82** (1999) 4930.
- [34] S. S. Banerjee, N. G. Patil, K. Ghosh, S. Saha, G. I. Menon, S. Ramakrishnan, A. K. Grover, P. K. Mishra, T. V. C. Rao, G. Ravikumar, V. C. Sahni, C. V. Tomy, G. Balakrishnan, D. Mck. Paul and S. Bhattacharya, Physica B **237-238** (1997) 315.
- [35] L. A. Angurel, F. Amin, M. Polichetti, J. Aarts and P. H. Kes, Phys. Rev. B **56** (1997) 3425 and references cited therein.
- [36] M. Isino, T. Kobayashi, N. Toyota, T. Fukase and Y. Muto, Phys. Rev. B **38** (1988) 4457.
- [37] H. Küpfer, Th. Wolf, C. Lessing, A. A. Zhukov, X. Lanon, R. Meier-Hirmer, W. Schauer and H. Wuehl, Phys. Rev. B **58** (1998) 2886 and references cited therein.
- [38] T. Nishizaki, T. Naito, and N. Kobayashi, Phys. Rev. B, **58** (1998) 11169.

- [39] R. Modler, P. Gegenwart, M. Lang, M. Deppe, M. Weiden, T. Luhmann, C. Geibel, F. Steglich, C. Paulsen, J. L. Tholence, N. Sato, T. Komatsubara, Y. Onuki, M. Tachiki and S. Takahashi, *Phys. Rev. Lett.* **76** (1996) 1292.
- [40] H. Sato, Y. Akoi, H. Sugawara and T. Fukahara, *J. Phys. Soc. Jpn.* **64** (1995) 3175.
- [41] C. V. Tomy, G. Balakrishnan and D. Mck. Paul, *Physica C* **280** (1997) 1.
- [42] C. V. Tomy, G. Balakrishnan and D. McK. Paul, *Phys. Rev. B* **56** (1997) 8346.
- [43] K. Hirata, H. Takeya, T. Mochiku and K. Kadowaki, *Advances in Superconductivity VIII*, edited by H. Hayakawa and Y. Enomoto (Springer-Verlag, Berlin, Germany, 1996) p. 619.
- [44] G. W. Crabtree, M. B. Maple, W. K. Kwok, J. Herrmann, J. A. Fendrich, N. R. Dilley and S. H. Han, *Physics Essays* **9** (1996) 628 and references cited therein.
- [45] H. Pastoriza, M. F. Goffman, A. Arribre, and F. de la Cruz, *Phys. Rev. Lett.*, **72** (1994) 2951.
- [46] E. Zeldov, D. Majer, M. Konczykowski, V. M. Vinokur and H. Shtrikman, *Nature*, **375** (1995) 373.
- [47] A. Schilling, R. A. Fisher, N. E. Phillips, U. Welp, D. Dasgupta, W. K. Kwok, G. W. Crabtree, *Nature*, **382** (1996) 791.
- [48] T. Sasagawa, K. Kishio, Y. Togawa, J. Shimoyama, and K. Kitazawa, *Phys. Rev. Lett.*, **80** (1998) 4297 and references therein.
- [49] M. J. W. Dodgson, V. B. Geshkenbein, H. Nordborg, and G. Blatter, *Phys. Rev. Lett.*, **80** (1998) 837.
- [50] T. V. Chandrasekhar Rao, M. J. Higgins, V. C. Sahni, G. Ravikumar, P. K. Mishra, S. S. Banerjee, N. G. Patil, S. Ramakrishnan, A. K. Grover, S. Bhattacharya, C. A. Scott, C. V. Tomy, G. Balakrishnan and D. McK. Paul (unpublished).
- [51] S. S. Banerjee, N. G. Patil, S. Ramakrishnan, A. K. Grover, S. Bhattacharya, G. Ravikumar, P. K. Mishra, T. V. Chandrasekhar Rao, V. C. Sahni, M. J. Higgins, *Appl. Phys. Lett.* **74** (1999) 126.
- [52] G. Ravikumar, P. K. Mishra and V. C. Sahni, S. S. Banerjee, A. K. Grover and S. Ramakrishnan, P. L. Gammel, D. J. Bishop and E. Bucher, M. J. Higgins and S. Bhattacharya, (unpublished).
- [53] G. Ravikumar, K. V. Bhagwat, V. C. Sahni, A. K. Grover, S. Ramakrishnan and S. Bhattacharya, (unpublished).
- [54] C. P. Bean, *Phys. Rev. Lett.*, **8** (1962) 250.
- [55] S. S. Banerjee, S. Saha, N. G. Patil, S. Ramakrishnan, A. K. Grover, S. Bhattacharya, G. Ravikumar, P. K. Mishra, T. V. C. Rao, V. C. Sahni, C. V. Tomy, G. Balakrishnan, D. Mck. Paul, M. J. Higgins, *Physica C* **308** (1998) 25.

FIG. 1. (a) Schematic vortex phase diagram for an ideal (pinning free) vortex array under the influence of thermal fluctuations (drawn following Ref.3). Note that the melting line separating the Abrikosov flux line lattice (FLL) from the vortex liquid phase has a reentrant character[4].

(b) Schematic vortex phase diagram for a vortex array under the combined influence of pinning centers and thermal fluctuations (drawn following Refs. 6-8). Note that the elastically pinned FLL (named as Bragg glass) is sandwiched between the dilute and dense glassy phases of vortex matter named as Reentrant glass[8] and vortex glass [6], respectively. The dotted B* line separating the Bragg glass and Vortex glass phases is believed to be pinning induced, whereas the solid lines(s) separating the vortex solid phase(s) and the vortex liquid phase is considered to be caused by thermal fluctuation effects.

FIG. 2. The temperature variation of the in-phase (χ') ac susceptibility ($h_{ac} \approx 1$ Oe (r.m.s.) and $f = 211$ Hz) of the cleanest crystal A of hexagonal 2H-NbSe₂ in nominally zero bias field (no vortex array) and in a dc field of 4 kOe (vortex array with $a_o \approx 790 \text{ \AA}$). In zero bias field, the normalized χ' response abruptly increases from -1 towards near zero value in the normal state; $\Delta T_c(0)$ value provides a measure of the width of the superconducting transition. In the dc field of 4 kOe, χ' shows a sharp negative peak due to peak effect (PE) phenomenon in J_c . Note that the sharpness of PE exceeds that of the superconducting transition. The inset focuses attention onto a paramagnetic peak due to differential paramagnetic effect (DPE) located at the edge of the PE peak. Note the recipe to locate the positions of onset temperature T_{pl} of PE, the temperature of PE peak T_p , the irreversibility temperature T_{irr} and superconducting transition temperature T_c .

FIG. 3. Magnetic phase diagrams (for $H > 1$ kOe) determined for samples A, B and C of 2H-NbSe₂ having progressively larger number of pinning centers. Note that in sample C, the lines marking the onset of PE (H_{pl}), the onset of reversibility (H_{irr}) and the upper critical field (H_{c2}) can be distinctly identified, whereas in sample A, the H_{pl} , the H_p and the H_{irr} lines are so close that it suffices to draw just the H_p line. For justification of nomenclature of different phases shown in this figure, see text.

FIG. 4. (a) Temperature dependence of χ' for vortex arrays created in zero field cooled (ZFC) and field cooled (FC) modes in a dc field of 5 kOe (H_{dc}/c) in sample C of 2H-NbSe₂. Note the occurrence of two sharp changes in χ' response at the onset temperature T_{pl} and peak temperature T_p in the ZFC mode. Further, the difference in χ' behavior between ZFC and FC modes disappears above the peak temperature of PE *a la spin glass phenomenon*.

(b) χ' responses showing irreversible behavior while thermal cycling across the onset and the peak positions of PE in sample C in a field of 5 kOe. The dotted and solid curves show χ' response recorded while warming up the vortex arrays created in ZFC and FC modes. The data points refer to χ' behavior recorded while cooling down from (i) $T_I < T_{pl}$ and (ii) ($T_{pl} < T_{II} < T_p$ and (iii) $T_{III} > T_p$. Note that while cooling down from T_I , the χ' retraces its behavior recorded while warming up, whereas while cooling down from T_{II} and T_{III} , the χ' response does not retrace its behavior recorded while warming up.

FIG. 5. Magnetic phase diagrams (for $H > 1$ kOe) for samples A, B and C of 2H-NbSe₂. Note that we have drawn only the loci of peak temperatures in all the three samples. In the field region of 0.5 to 1 kOe, the PE peak in sample C is also so sufficiently narrow that it suffices to draw only the locus of peak temperatures in it. However, as the field decreases below 500 Oe, the PE peaks in sample B and C start to broaden considerably. The $t_p(H)$ curve in sample B clearly shows a turnaround characteristic at $H \sim 100$ Oe. In sample A, the $t_p(H)$ curve can be seen to be on the verge of turning around at $H \sim 50$ Oe.

FIG. 6. Log-log plots of J_c vs H at selected temperatures in sample B (Figs. 6(a) to 6(d)) and sample C (Figs.6(e) to 6(h)) of 2H-NbSe₂. The peak fields H_p have been marked in Figs.6(a) to 6(c) and Figs.6(e) to 6(g). The insets in Figs.6(c) and in 6(g) show the plots of $t_p(H)$ ($= T_p(H)/T_c(0)$) and $t_c(H)$ ($= T_c(H)/T_c(0)$) curves in samples B and A, respectively. The data points on respective $t_p(H)$ curves identify the temperature values at which the J_c vs H curves have been displayed in the main panels. Figs.6(a) and 6(e) show how the entire field span can be subdivided into three different pinning regimes (see text for details). Note that in Figs.6(d) and 6(h), the $J_c(H)$ monotonically decays with H and the peak effect phenomenon cannot be distinctly discerned.

FIG. 7. Log-log plots of $J_c(H)/J_c(0)$ vs H/H_{c2} at selected temperatures in sample A (Fig.7(a)) and in sample B (Fig.7(b)) of 2H-NbSe₂. The power law regime and the PE region have been marked at the lowest reduced temperatures of 0.973 and 0.965 in samples A and B, respectively. Note that in both the samples, the field span over which the power law dependence holds reduces as t increases. The normalized current density reaches upto a limiting value at the peak of PE. At the lowest field end, the normalized current density flattens out to the small bundle pinning limit.

FIG. 8. Magnetic phase diagram in the low field and high temperature region in crystals A, B and C of 2H-NbSe₂. The H-T region between the onset of PE (H_{pl} line) and the H_{c2} boundary has been shaded by dotted lines and the region below the onset of power law regime has been shaded by solid lines in all the three samples. Note that the collectively pinned power law regime is sandwiched between the so-called re-entrant disordered region and the amorphous region for $0.97 < t < 0.995$ in crystal A, for $0.95 < t < 0.98$ in crystal B and for $0.8 < t < 0.95$ in crystal C. At temperatures above the turnaround features in $H_{pl}(t)$ curves, the vortex array remains in a disordered state over the entire field range.

FIG. 9. Temperature variation of χ' for vortex arrays created in ZFC and FC modes in fields of 10 kOe and 33 kOe in single crystals of $Ca_3Rh_4Sn_{13}$ (Fig.9(a)) and YNi_2B_2C (Fig.9(b)), respectively. Note the occurrence of the sharp transition in χ' response in ZFC mode at temperatures T_{pl} and T_p , respectively in both the crystals. As in Fig. 4(a), the difference in χ' behavior between ZFC and FC modes disappears above the peak temperature T_p .

FIG. 10. Magnetic phase diagrams in crystals of $Ca_3Rh_4Sn_{13}$ (Fig.10(a)) and YNi_2B_2C (Fig.10(b)). The nomenclature of different phases shown in these diagrams follows the prescription justified for 2H-NbSe₂ system in Fig.3.

FIG. 11. A quasi-schematic plot of the magnetic phase diagram in a weakly pinned type II superconductor (here, for example, crystal B of 2H-NbSe₂). Different vortex states are shown sandwiched between H_{c1} and H_{c2} lines. This diagram has been drawn following analysis of experimental data on current density in contrast to the schematic shown in Fig. 1(b) on the basis of theoretical simulations. The similarities in the two diagrams attest to the appropriateness of the nomenclature of different phases in Fig. 11.

Fig.1(a) S. S. Banerjee et al

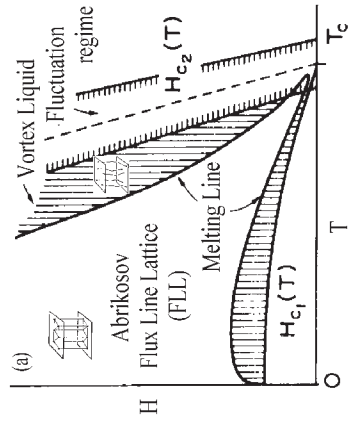
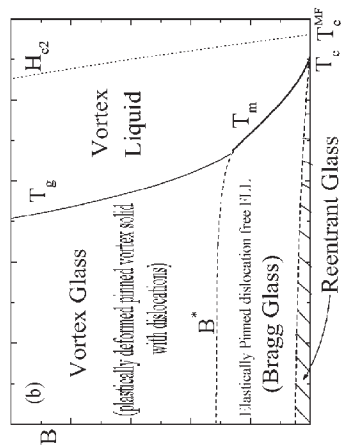


Fig. 1(b) S. S. Banerjee et al



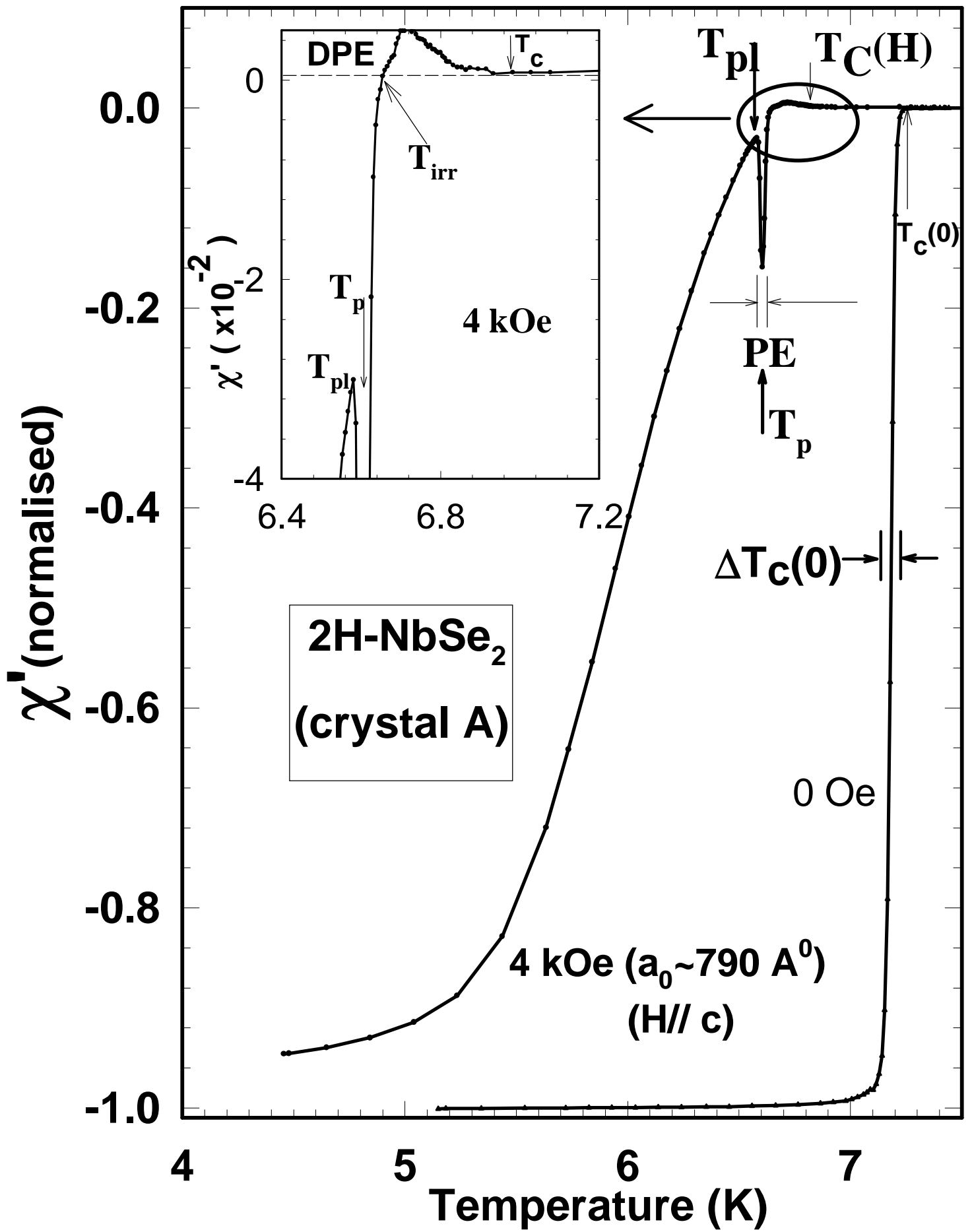


Fig.2. S. S. Banerjee *et al*

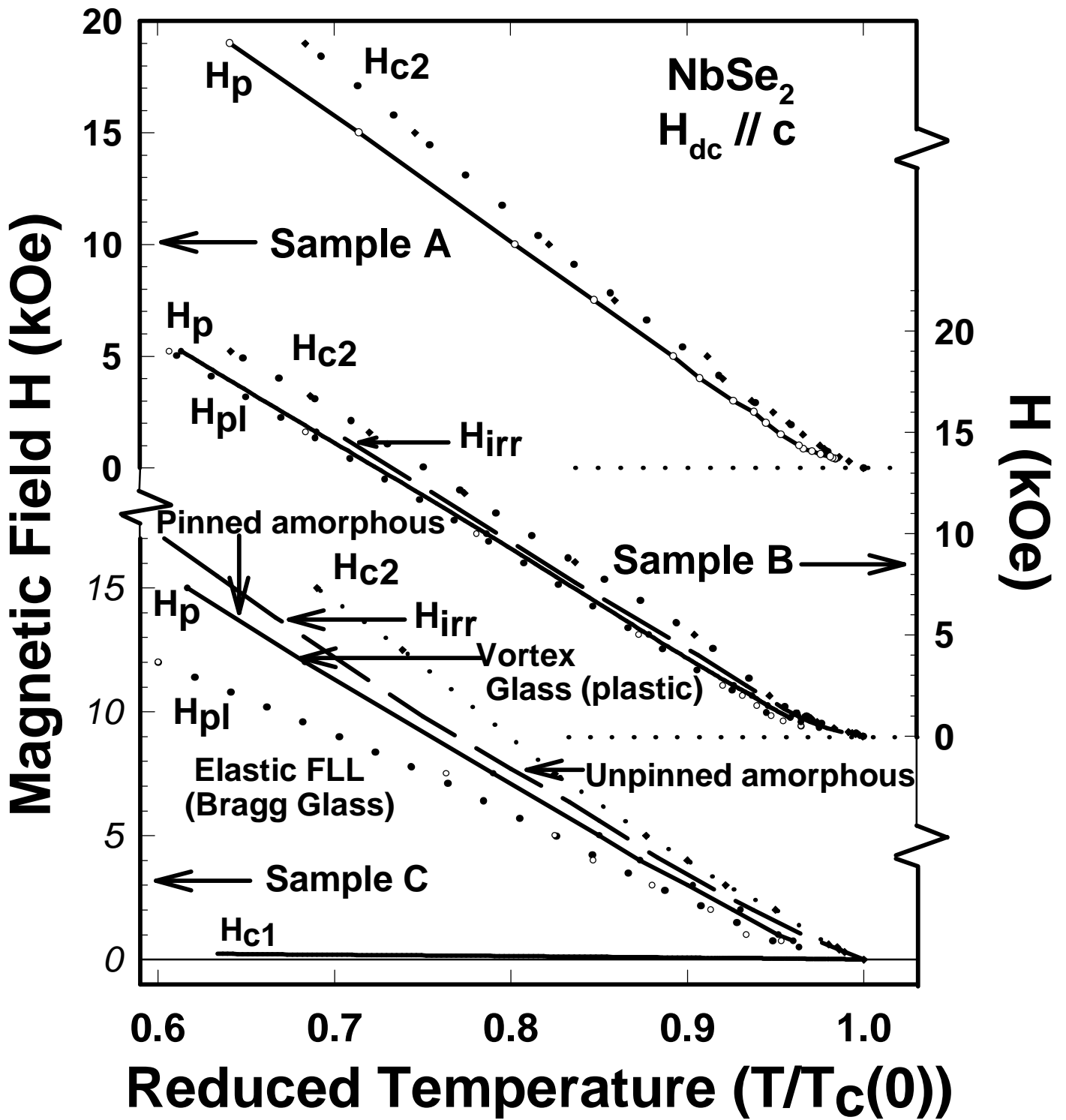


Fig.3. S. S. Banerjee et al

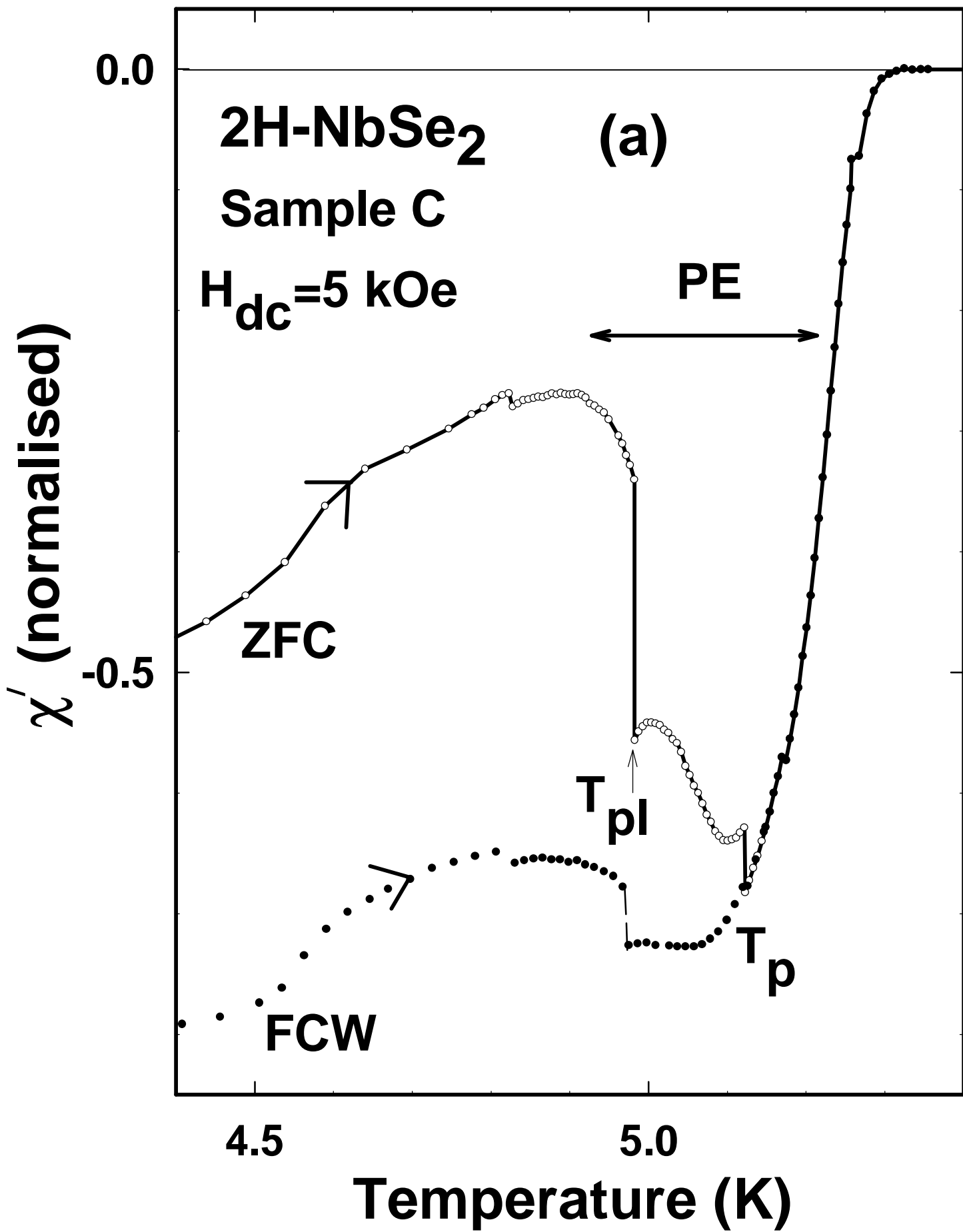


Fig.4(a) S. S. Banerjee

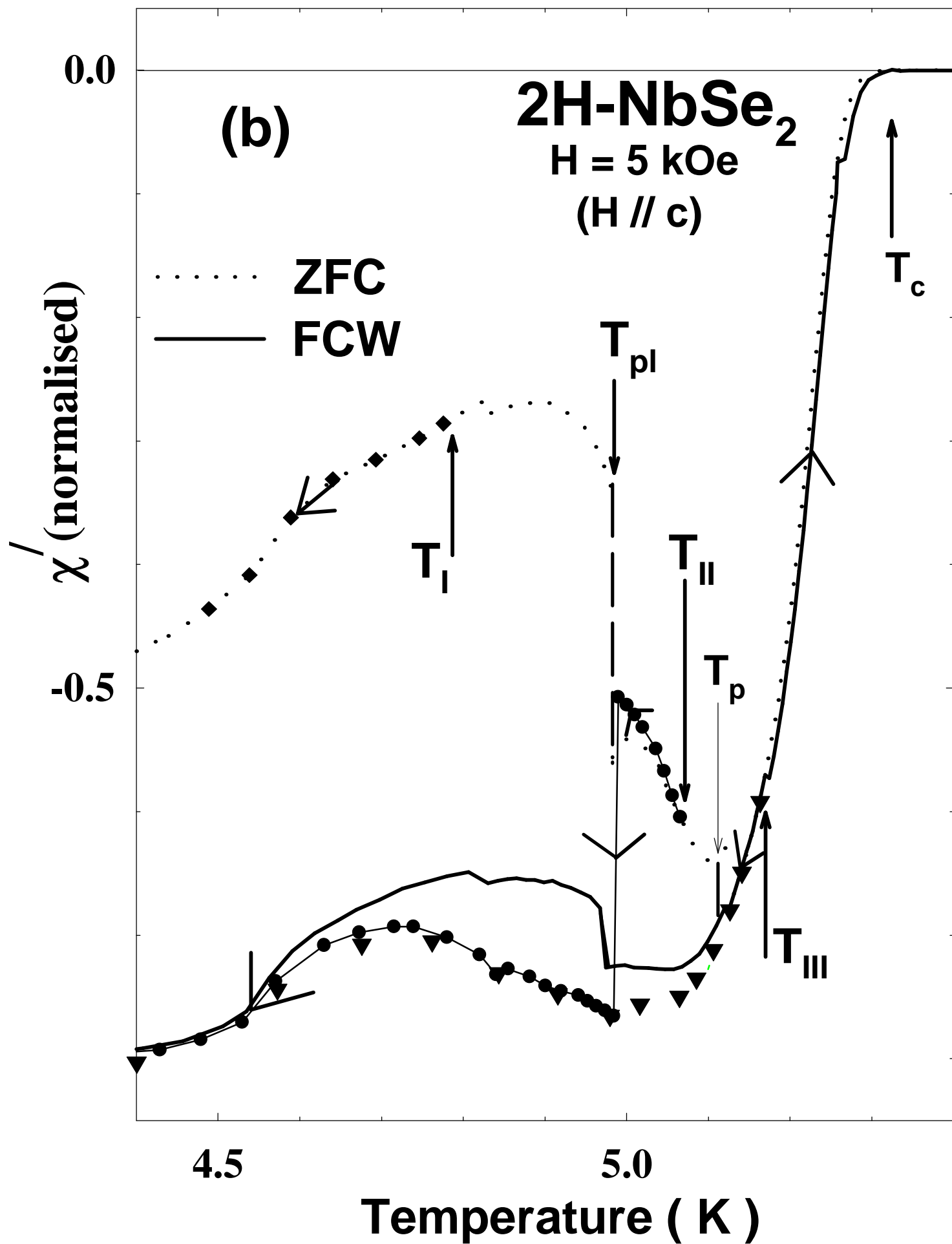


Fig.4(b) S. S. Banerjee et al

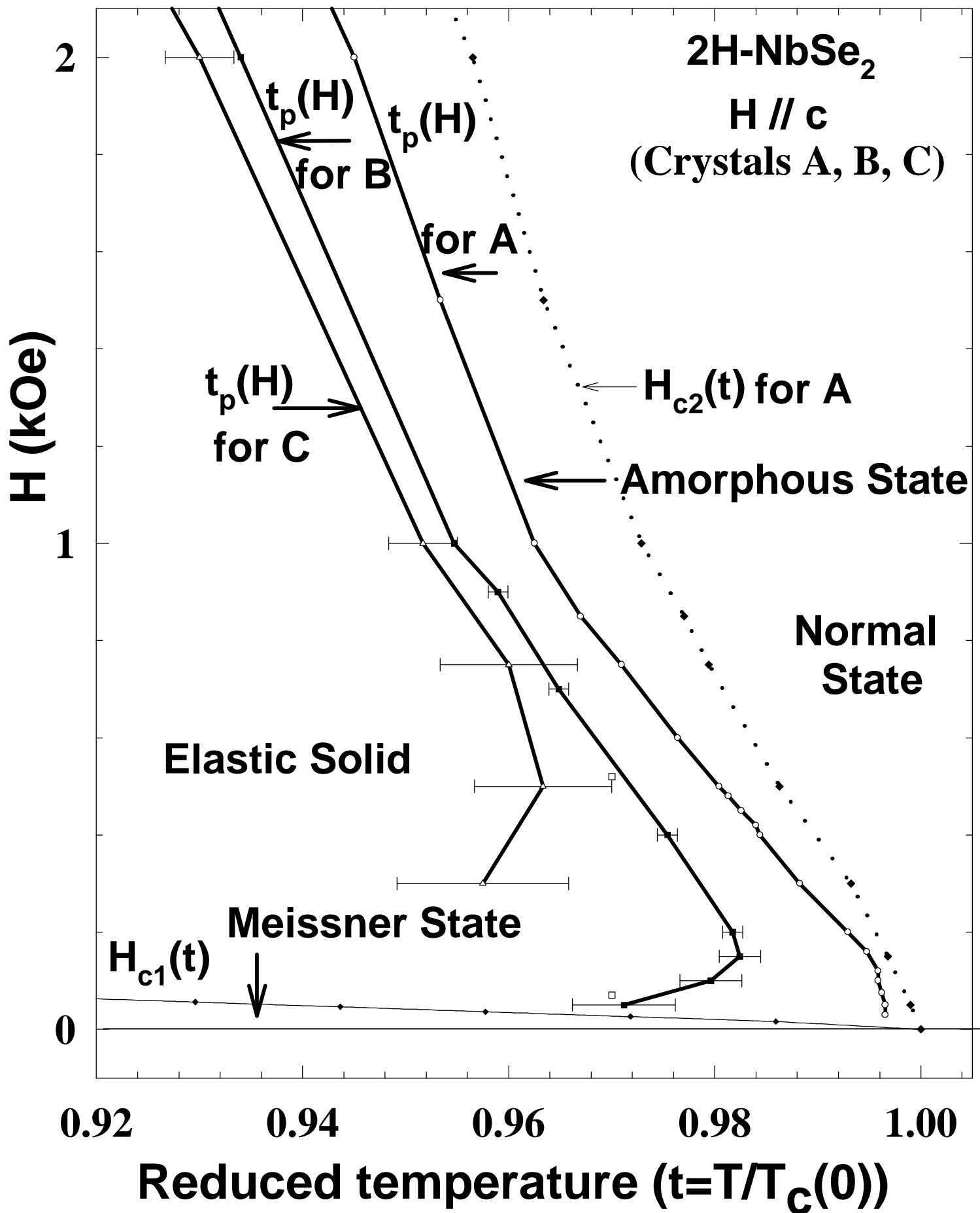


Fig.5 S. S. Banerjee et al

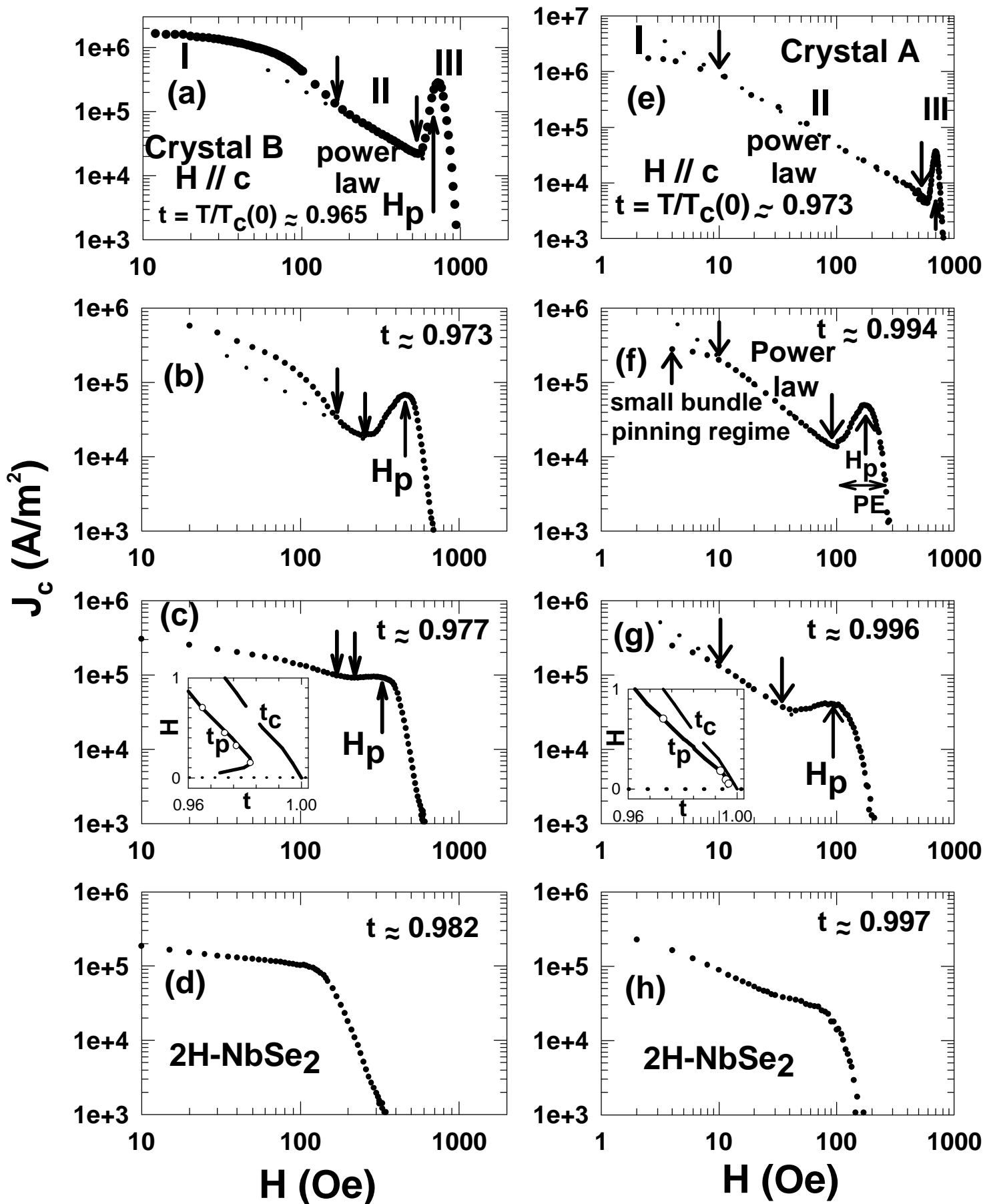


Fig.6. S. S. Banerjee et al

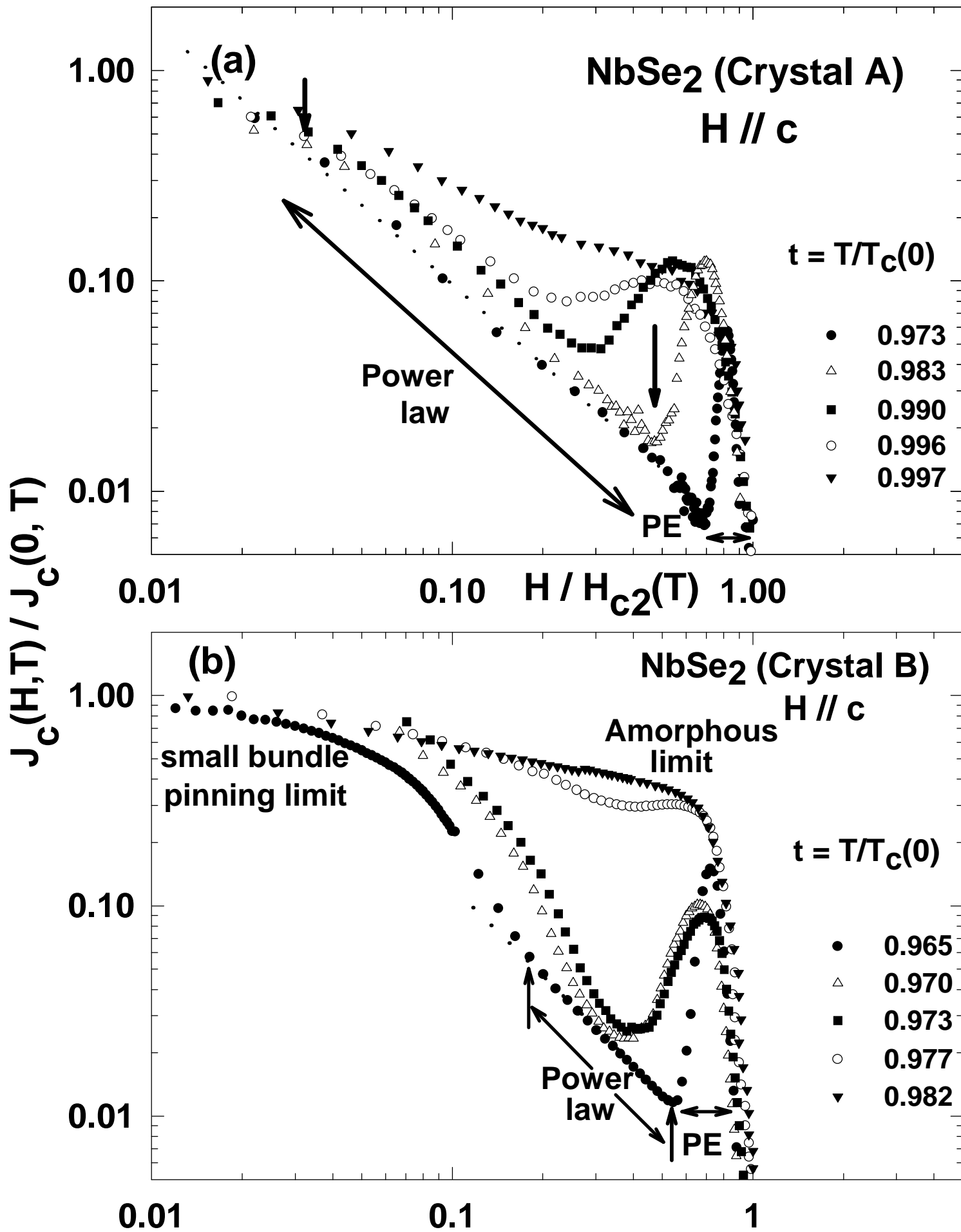
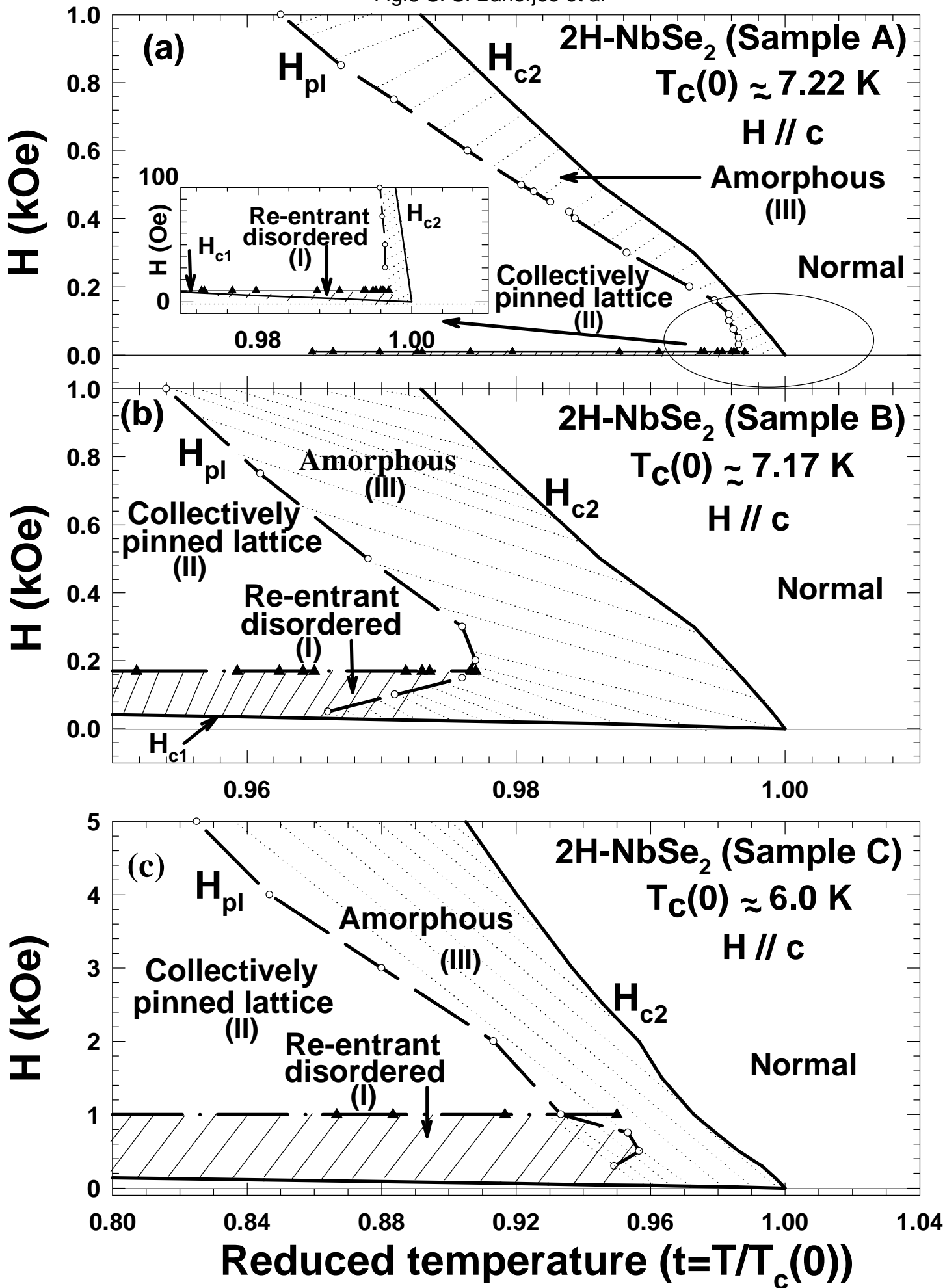


Fig.7 S. S. Banerjee et al



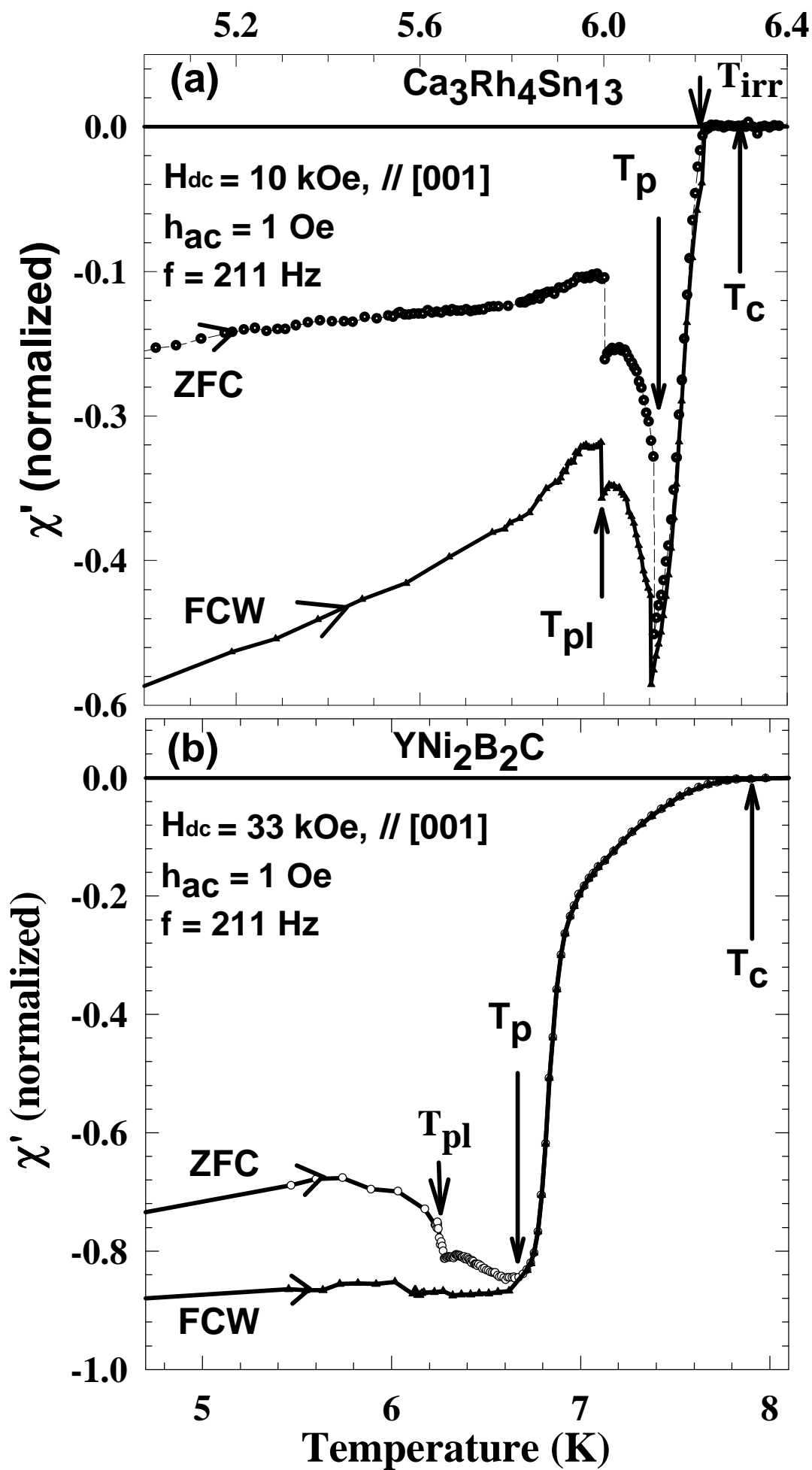


Fig. 9 S. S. Banerjee et al

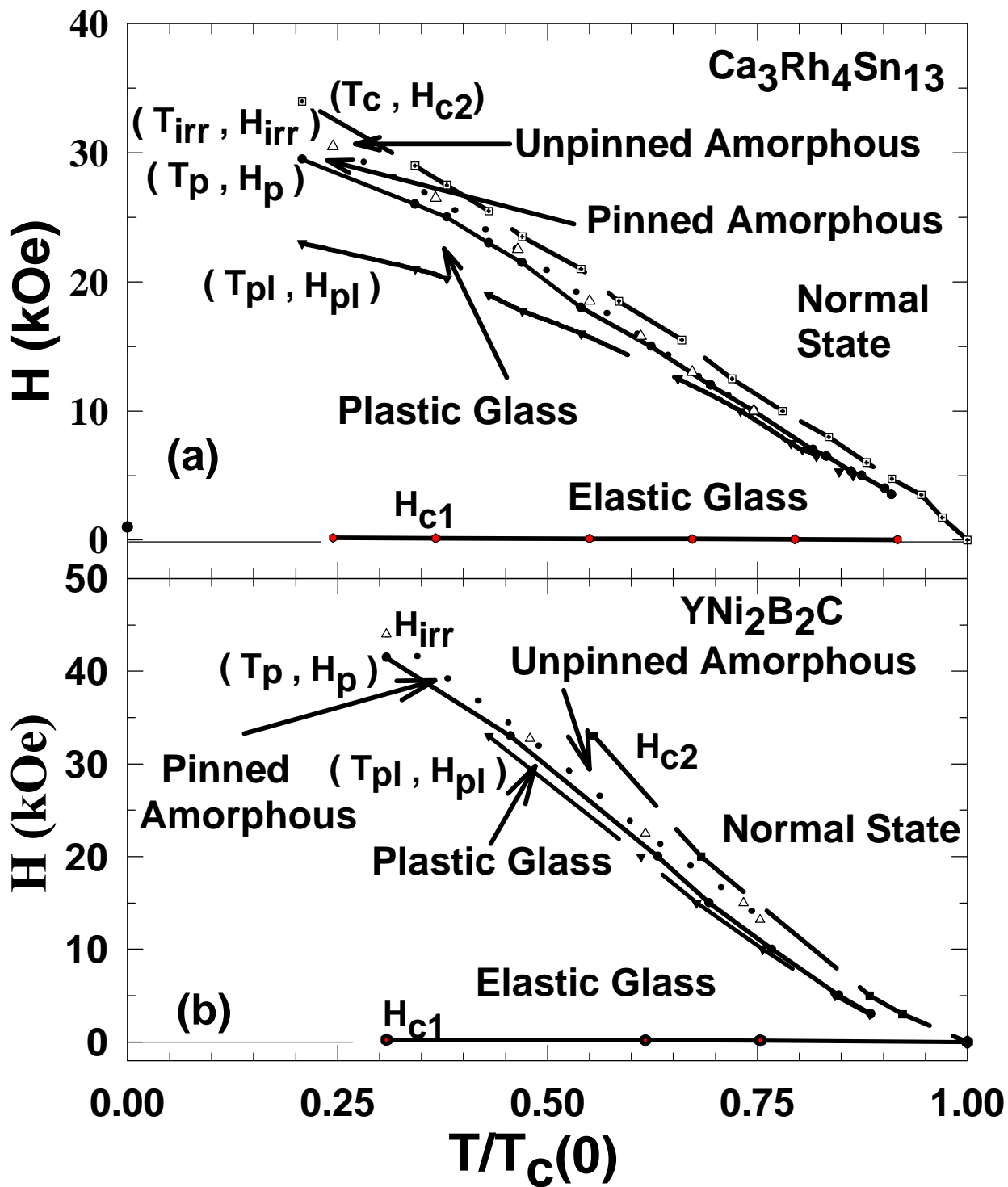


Fig. 10 S. S. Banerjee et al

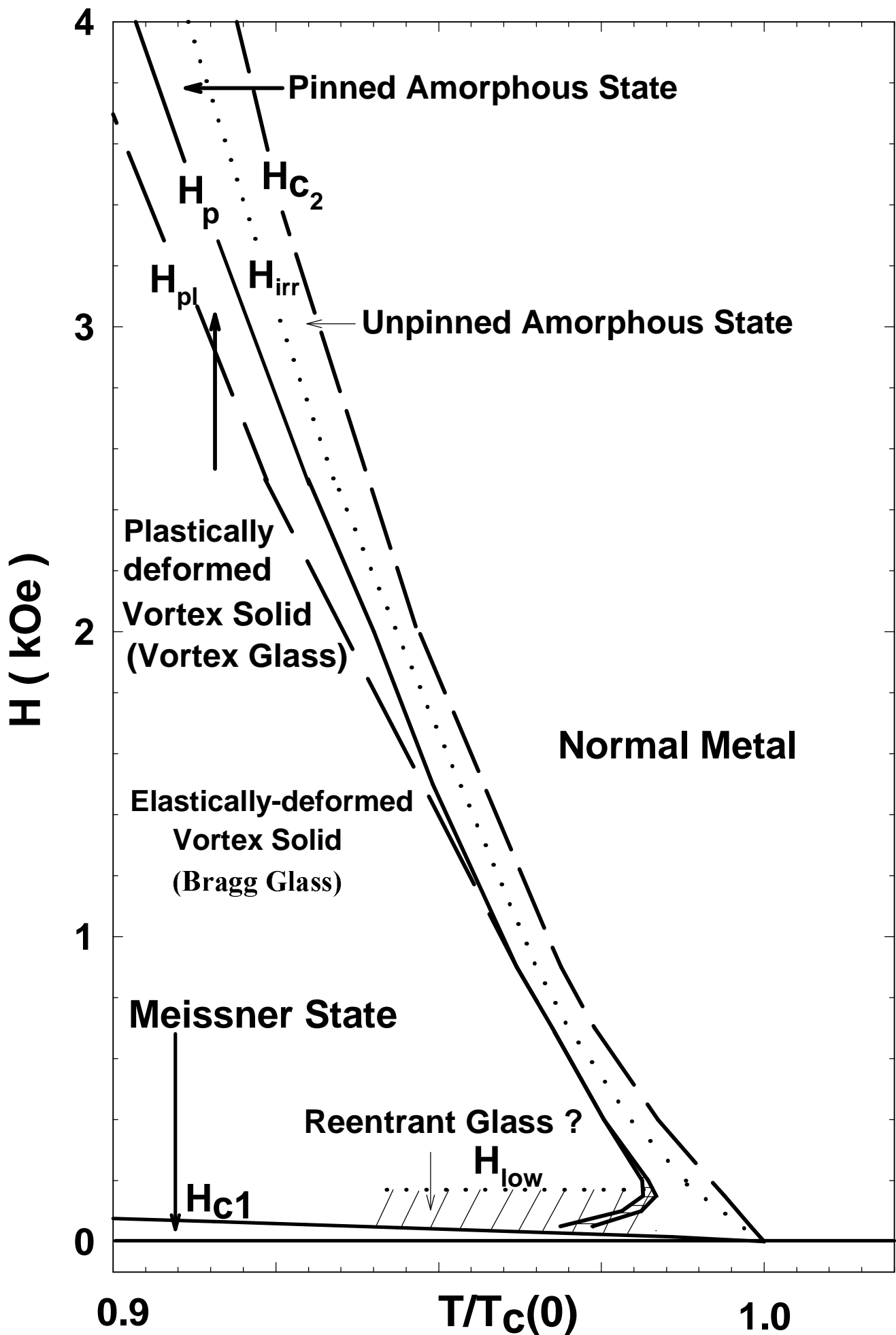


Fig.11 S. S. Banerjee et al